J. Water Environ. Nanotechnol., 4(1): 67-74 Winter 2019

ORIGINAL RESEARCH PAPER

Template assisted Synthesis of tin oxide nanostructures electrodes by using nanoporous alumina template for detection of toxic chemicals in water such as hydrazine

Ghaffar Torkashvand, Norodin Mirnia*, Ali Bahari

Department of Solid State Physics, University of Mazandaran, Babolsar, Iran

Received: 2018-08-27 Accepted: 2018-10-01 Published: 2019-02-01

ABSTRACT

Template-assist method is one of the most important techniques for synthesize nanostructures , because of more parameters that can be change to fabricate different nanostructures with desired nano-scale features. self- ordered anodic alumina is one of the most important honeycomb structure that can be used as a template. by using self-ordered nanoporous as a template and hydrothemal process as a deposition technique,different structures like nanowire,nanotube and nanoparticle was fabricated. The effect of surfactant and temperature on the formation of various nano-structures were investigated by SEM (scanning electron microscopy) and EDX (Energy dispersive x- ray) analysis. Electrical properties and I(Current)- Voltage (V)- Gate- source behavior of the samples was measured by four-probe (4- probes) method. Tin oxide nanoparticle array on the surface of alumina membrane used as chemical sensor in case of detecting hydrazine. The obtained results indicate that Alumina doped with tin oxide nanoparticle is suitable for detection of toxic chemicals in water such as hydrazine.

Keywords: *Hard Anodization; Hydrothermal Method; Nanoporous Anodic Alumina; Nanostructures; Surface Modification*

How to cite this article

Torkashvand G, Mirnia N, Bahari A. Template assisted Synthesis of tin oxide nanostructures electrodes by using nanoporous alumina template for detection of toxic chemicals in water such as hydrazine . J. Water Environ. Nanotechnol., 2019; 4(1): 67-74. DOI: 10.22090/jwent.2019.01.007

INTRODUCTION

A chemical sensor is a self-contained analytical device that can provide information about the chemical composition of its environment, that is, a liquid or a gas phase. The information is provided in the form of a measurable physical signal that is correlated with the concentration of a certain chemical species (termed as analyte). The contact area of the device is a key factor in case of the detection process, so much affords were done to increase the contact area of the device to promote the performance of them. In this case, nanostructure materials such as nanotubes, nanofilms, nanoparticles and nanoporous because of their high surface area to volume ratio are the most common candidates for sensing device. Nanoporous materials have significant advantages to other nanostructures, such as thermal and chemical stability, constant form, low cast synthesis, easy handle and controllable porosity.

Nanoporous Anodic Alumina (NAA) is the most recognized nanoporous but on the other hand, it has low sensitivity and selectivity, so the surface wall of this structure should be functionalized in case of increasing sensitivity and sensing different analytes. NAA is mainly sensitive to ammonia and humidity [1–5], many affords were done to promote the selectivity of NAA and make it sensitive to different analytes, such as dopingNAA with nanoparticles, nanorods, and nanotubes on

* Corresponding Author Email: *snmir@umz.ac.ir*

the surface and inner wall of pores[6]. The growth of carbon nanotubes on the surface of nanoporous alumina improved the sensing property and storage capability of hydrogen gas[6,7]. Using polymer as coverage of NAAnanopores array was investigated in case of drug and biomaterial sensor[8–13]. Synthesis of nanorods and nanoparticles on the wall of NAA is another strategy to increase adsorption and interaction of analytes by NAA[14-22].

After introducing the two-step mild anodization technique by Masuda and Fukuda [23], nanoporous aluminum oxide was widely used as a practical template to fabricate the nanoscale porous structure. Although this technique requires long time processing, it provides self-ordering in narrow interpore distances by applying the certain anodization voltage and electrolyte solutions desired in industrial applications. Many efforts have been done to extend the range of the pore size and interpore distances of the self-ordered NAA templates. To accelerate fabrication of highly self-ordered porous aluminum oxide template with a wide range of pore size and interpore distances, hard anodization (HA) technique based on the high current density was reported. Potentials are higher than the conventional potentials used for sulfuric, oxalic acids in the mild anodization regime. An optimum self-ordering was achieved in a wide range of interpore distances from 130 to 270nm.

The hydrothermal method has some advantages over another method of synthesis nanomaterial, in this method, many of metal oxide nanomaterials can be synthesized and large size nanostructures is achievable by changing condition, also this method can be combined with others methods in case of template-assisted synthesis24.

Tin dioxide is a transparent conducting oxide and a wide bandgap n-type semiconductor has been used in many applications such as gas sensors, solar cells, supercapacitors, and batteries.

Tin oxide can be synthesized using a variety of techniques such as sol-gel, hydrothermal method, precipitation. Combining of these methods with hard templating method led to less agglomeration that provides smaller particle sizes and larger surface area, which makes them suitable for applications such as gas sensors, electrode materials for supercapacitors and batteries as compared to microemulsions techniques.

The unique chemical and physical properties of one-dimensional (1D) nanomaterials (nanorods, nanowires, and nanotubes) have presented new opportunities in the miniaturization of devices. Compared to nanoparticles, 1D nanomaterials offer more varied possibilities in constructing 2D and 3D geometries, which can then be used to build more complex Nanodevices. Fewer reports are found for the synthesis of 1D nanomaterials than for the nanoparticles perhaps due to the difficulty in constructing anisotropic structures.

It was suggested that embedding the active material (tin oxide) in a less active matrix (NAA) serving as oxidant agent would improve the electrode sensitivity. In this work, these two methods will be combined to design novel nanoscale Sn-based electrodes hopefully with high sensitivity and satisfactory stability.

The motivation of this work is to inject some guest impurity to NAA for increasing sensibility and selectivity of absorbent material in case of sensing procedure. In this case, the tin oxide was deposited on to NAA wall as a guest material to improve sensing property of nanopore array. The hydrothermal method was chosen to the growth of nanosized tin oxide on the surface of NAA but unlike conventional hydrothermal method at high pressure, this process performed at ambient pressure. This selected impurity led to oxidation of hydrazine in case of electrochemical sensing.

EXPERIMENTS

Alumina membranes

Samples with a radius of 8mm were cut from a high purity foil of aluminum (99.999% purity, 0.3mm thickness), degreased in acetone, and washed in deionized water. Before anodization, the aluminum was electropolished at a constant current density ($100mAcm^{-2}$) in a 1:4 volume mixture of perchloric acid and ethanol at room temperature to diminish the roughness of the aluminum foil surface. The hard anodization (HA) technique was applied to aluminum foil in 0.3M oxalic acid as electrolyte. During the anodization process, vigorous steering was applied and the electrolyte temperature was kept constant at 0°C. To create a protective layer against burning at high voltages, the procedure was started with an initial voltage 40V and after 500 seconds, the anodization voltage was increased with the rate of $0.5Vs^{-1}$ to a final constant potential 130V, anodization continued for 25minutes. Fig. 1 shows the time evaluation of voltage and current of the anodization process. The relationship between pore diameter (D_p) and the applied voltage is linear($D_p=\lambda_p V$) in case of hard

anodization $\lambda_p \approx 0.4$[25], so the average pore diameter is 52 nm and the thickness of NAA layer is about 25 µm. After the anodization process, to extend the pore size of NAAtamplates in order to get higher surface charges, they were immersed in phosphoric acid 0.5M at 30ºC for 30 minutes[26,27]. The second type of membrane was synthesized by doping Sn in NAAmembraneduring anodization process, in this case after the first peak of anodization, 30mL of 0.02M $SnCl_2 \cdot 2H_2O$, was added to oxalic acid solution and anodization continued under vigorous stirring. The final current of anodization, in this case, is higher than regular anodization, so the growth rate of the doped NAA layer is higher than the pure NAA layer. In this condition, the thickness of the NAA layer is about 40 µm.2.2. Hydrothermal process.

By using $SnCl_2 \cdot 2H_2O$ as a precursor with a different surfactant, three solutions were prepared to synthesis nanostructure in presence of NAA templates. In the first case(T type), the precursor solution was prepared by dissolving 1.2g of $SnCl_2 \cdot 2H_2O$ and 2g NaOH pellets in 50mL deionized water under vigorous stirring then 1.4g of Hexamethylenetetramine ($C_6H_{12}N_4$) were added which were stirred until NaOH dissolved, after that, it was maintained at 200ºC for 4h. In the second case(W type), 1.2g $SnCl_2 \cdot 2H_2O$ was dissolved into 45mL distilled water under continuous magnetic stirring, Subsequently, 5mL of 30% H_2O_2 and 2g NaOH pellets were added under vigorous stirring until NaOH dissolved and it was maintained at 200 ºC for 4h. In the third case(P-type), 1.2g $SnCl_2 \cdot 2H_2O$ was dissolved in 40mL of distilled

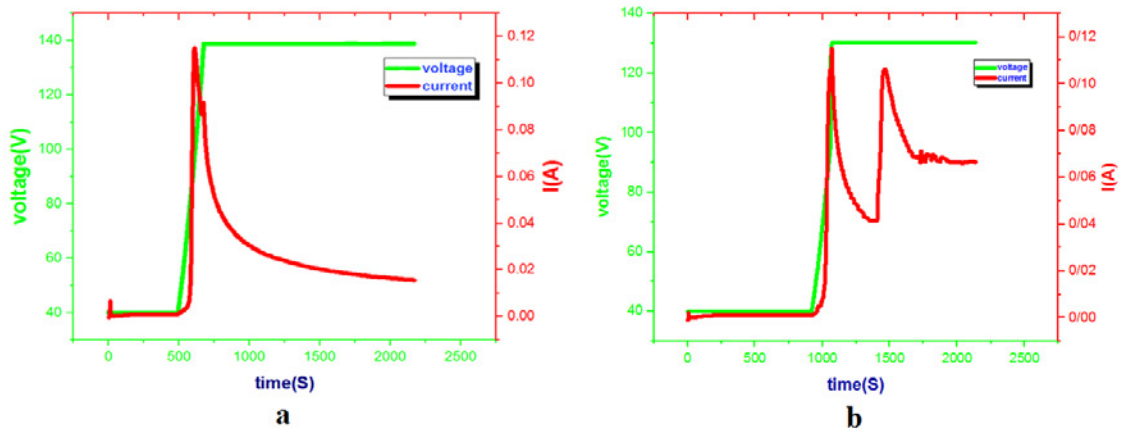

Fig. 1. Graph of voltage(V) and current(I) vs time(s) during anodization process (a)in oxalic acid (b) in mixture of oxalic acid and tin chloride

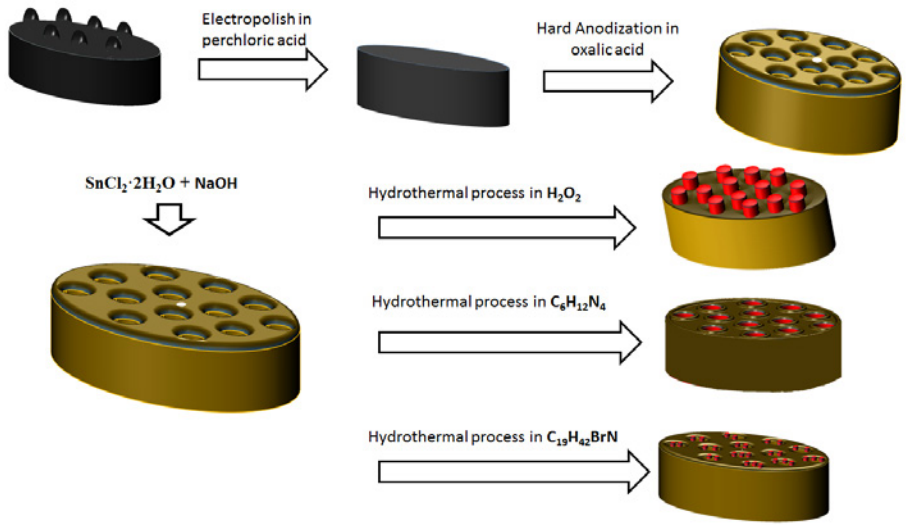

Fig. 2. Schematic of whole synthesis method of tin oxide-alumina nanocomposite

water then 2g NaOH pellets were dissolved in 10mL of distilled water and it was added drop-wise to the solution then 2g CTAB ($C_{19}H_{42}BrN$) was put into the above solution under stirring for 1h then it was maintained at 90°C for 4h. After washing the samples several times in distilled water and ethanol and a mixture of 0.5 M phosphoric acid and 0.5 M hydrochloric acid respectively, all of the samples were dried at 70°C for 1h. The schematic of all synthesis stages is depicted in Fig. 2 and morphology and structural formula of the different SnO_2-doped NAA composite materials was determined by FESEM and EDX analysis as shown in Figs. 3&4.

RESULTS AND DISCUSSION

It appears that change of surfactant species have a significant effect on the shape of SnO_2 nanostructures that grows on the surface of NAA templates. In order to evaluate the effect of hydrothermal condition on the shape of SnO_2 nanostructure, the hydrothermal preparation was carried out by changing the type of surfactant content. Fig. 3 shows the EDX graph and the weight percent of Sn in three nanostructures obtained after hydrothermal treatment. It appears that the SnO_2 doped sample showed different weight percent due to the different condition that SnO_2 was prepared. Fig. 3a shows the EDX graph of P-type sample, the weight percent of Sn, in this case, is 0.83%, it implies partial coverage of NAA template with Sn. on the other hand as shown in fig 2b for T type structure, the weight percent of Sn is 1.50%, so the coverage of NAA template is complete and nanotubes have been formed on the surface of NAA pores. In the case of W type structure as shown in fig 3c, the weight percent of Sn is 3.10%, so NAA pores completely filled and nanowires array have been formed inside of NAA template.Fig.3d shows the EDX graph of Sn-doped NAA during anodization, the weight percent of Sn, in this case, is 0.93%.

Fig.4 shows the FESEM cross-section images of SnO_2 doped NAA templates, where SnO_2 nanostructures were prepared under different condition. Fig. 4a is a cross-section image of Sn-doped NAA that doping was performed during

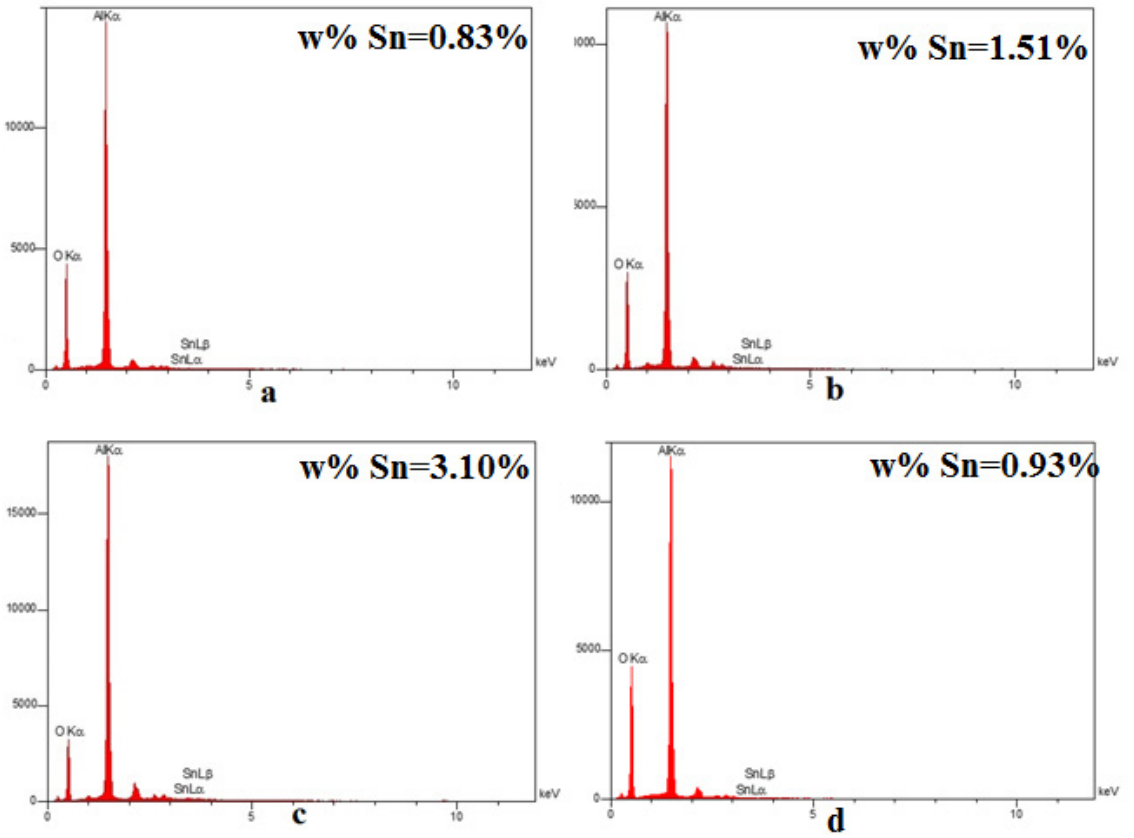

Fig. 3. EDX graph NAA (a) doped Sn during anodization. after hydrothermal process (b) p-type sample with 0.83%W Sn, (c) T-type sample with 1.51%W Sn, (c) w-type sample with 3.10%W Sn

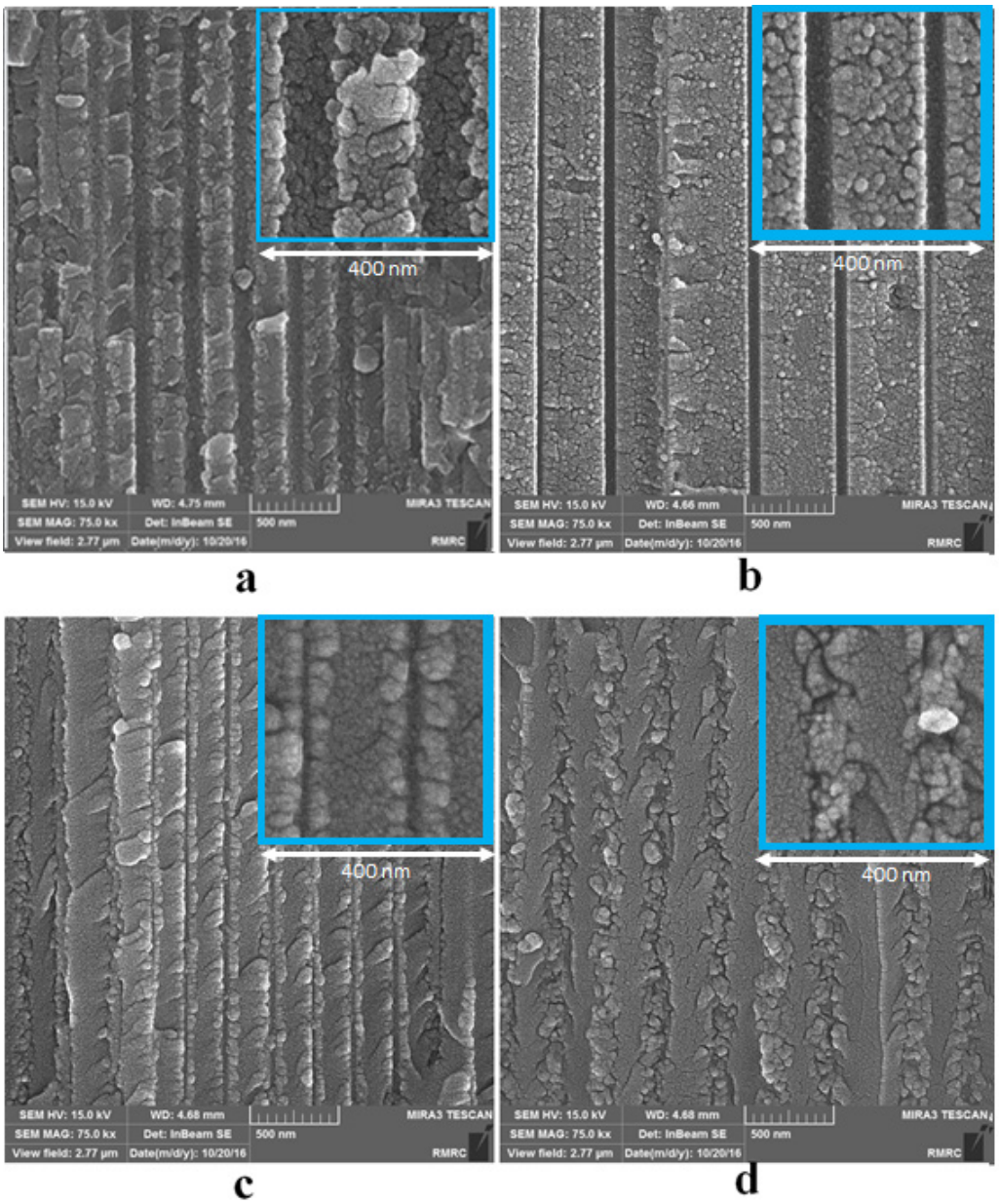

Fig. 4. Cross section FESEM image of alumina doped with (a) Sn during anodization process. (b) tin oxide nanoparticle(p-type). (c) tin oxide nanotube(t-type). (d) tin oxide nanowire(w-type)

the anodization process under hard anodization conditions without any modification.Fig.4b shows nanowire structures that have been formed inside of NAA pores after the hydrothermal process at 200ºC for a solution that containing H_2O_2(W type) with diameters equal to a pore diameter of NAA (approximately 130nm). Fig.4c shows hollow structures that cover the surface of NAA, the nanotube structures have been formed in a solution that containing Hexamethylenetetramine (T type), suggesting that the shape of SnO_2 nanostructure can be controlled by changing the type of surfactant. Fig.4d shows that nanoparticles with average size of 20nmhave been formed on the surface of the NAA in a solution containing CTAB at 90ºC (P-type). In case of comparing electrical properties of these nanostructures, all samples were used as a field effect transistor so that the alumina template is gate dielectric and the tin oxide layer is n-type channel. The variation of source-drain current respect to

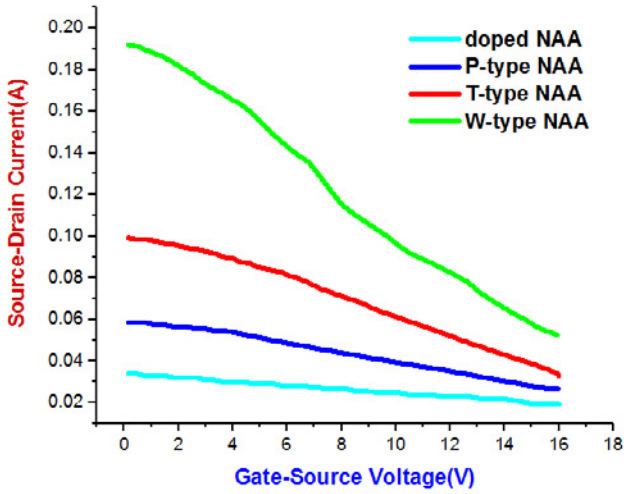

Fig. 5. Source-drain current versus gate-source voltage for different alumina-tin nanocomposite

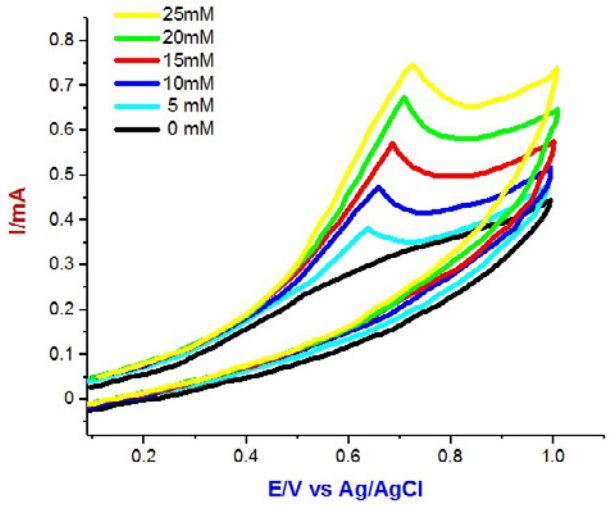

Fig. 6. Cyclic voltammograms of a NAA modified electrode(P type) at 50 mV/s in the absence and presence of 5, 10, 15, 20 and 25 m mol/ L hydrazine

gate-source voltage for all samples was investigated by using four probe technique. Alumina is a very good electrical insulator, so for comparing electrical properties of all samples, a relatively high voltage was applied to source-drain in order of measurable current for all transistor. By changing the gate-source voltage, the source-drain current was measured while the source-drain voltage kept at 100V. Fig.5 shows the graph of the source-drain current versus gate-source voltage. Doped NAA is the sample that doped whit Sn during anodization without hydrothermal process, in this case despite of higher percentage of Sn relative to P-type structure (as seen in Fig.3) the drain current is lower, it is because of injection of Sn inside of NAA whereas in the case of P-type structure, the tin oxide nanoparticles array is formed on surface of NAA so this semiconductor layer acts as a transistor channel . The w-type structure shows a higher drain current relative to T-type structure, it is maybe happened because of more homogeneity and the higher weight percent of Sn in the nanowire layer relative to the nanotube layer.

The last type of nanostructure (P-type) that contains tin oxide nanoparticles on the surface of NAA template is a preferable candidate for chemical sensors because of higher surface area to volume ratio, open pores and surface deposition of tin oxide

on the wall of NAA. So tin oxide nanoparticles array was chosen to detect toxic chemicals in water so cyclic voltammetry of this sample to hydrazine with scan rate 50 mV was performed by changing concertation of hydrazine from 5 mM to 25 mM as shown in Fig. 6. The oxidation peak of hydrazine in 0.7 volts, increases with increasing concentration of hydrazine, the amount of oxidation peak makes this sensor applicable for hydrazine detection within an intermediate range of hydrazine concentration.

CONCLUSION

Tin oxide nanotubes, nanowires, and nanoparticles arrays were synthesized using a template-assist synthesis of nanomaterials in NAA template combined with the hydrothermal method in different surfactant. By using this template-assist method the size and thickness of hollow structure shell was decreased (by conventional hydrothermal method, the size of hollow microspheres and thickness of shell is 2-3 μm and 60–140 nm respectively[28], while in case of template-assist method the size of hollow structure is about 300 nm and the thickness of shell is less than 100 nm). Furthermore, the diameter and length of nanorods were increased(by using the conventional hydrothermal method, diameter and length of nanorods are 10 nm and 50 nm respectively, while in the template-assist method the diameter and length of the nanowire is about 300 nm and 25 μm respectively). Because of high Surface to volume ratio, the nanoparticles array was used as a hydrazine sensor, Furthermore, field effect transistor sensor based on tin oxide nanowire arrays can be used as a gas sensor because of high sensitivity to gate-source voltage. Nanotubes and nanowires array also can be used as a chemical sensor by more modification such as widening nanotubes or removing alumina substrate.

CONFLICT OF INTEREST

The authors declare that there are no conflicts of interest regarding the publication of this manuscript.

REFERENCES

1. Varghese OK, Gong D, Dreschel WR, Ong KG, Grimes CA. Ammonia detection using nanoporous alumina resistive and surface acoustic wave sensors. Sensors and Actuators B: Chemical. 2003;94(1):27-35.
2. Dickey E, Varghese O, Ong K, Gong D, Paulose M, Grimes C. Room Temperature Ammonia and Humidity Sensing Using Highly Ordered Nanoporous Alumina Films. Sensors. 2002;2(3):91-110.
3. Sharma K, Islam SS. Optimization of porous anodic alumina nanostructure for ultra high sensitive humidity sensor. Sensors and Actuators B: Chemical. 2016;237:443-51.
4. Saha D, Ghara DK, Pal M. Nanoporous γ-alumina based novel sensor to detect trace moisture in high temperature and high pressure environment. Sensors and Actuators B: Chemical. 2016;222:1043-9.
5. Chen SW, Khor OK, Liao MW, Chung CK. Sensitivity evolution and enhancement mechanism of porous anodic aluminum oxide humidity sensor using magnetic field. Sensors and Actuators B: Chemical. 2014;199:384-8.
6. Agonafer DD, Oruc ME, Chainani E, Lee KS, Hu H, Shannon MA. Study of ionic transport through metalized nanoporous membranes functionalized with self-assembled monolayers. Journal of Membrane Science. 2014;461:106-13.
7. Ding D, Chen Z, Rajaputra S, Singh V. Hydrogen sensors based on aligned carbon nanotubes in an anodic aluminum oxide template with palladium as a top electrode. Sensors and Actuators B: Chemical. 2007;124(1):12-7.
8. Steinhart M. Polymer Nanotubes by Wetting of Ordered Porous Templates. Science. 2002;296(5575):1997-.
9. Feng CL, Zhong XH, Steinhart M, Caminade AM, Majoral JP, Knoll W. Graded-Bandgap Quantum- Dot-Modified Nanotubes: A Sensitive Biosensor for Enhanced Detection of DNA Hybridization. Advanced Materials. 2007;19(15):1933-6.
10. Santos A, Macías G, Ferré-Borrull J, Pallarès J, Marsal LF. Photoluminescent Enzymatic Sensor Based on Nanoporous Anodic Alumina. ACS Applied Materials & Interfaces. 2012;4(7):3584-8.
11. Kumeria T, Kurkuri MD, Diener KR, Parkinson L, Losic D. Label-free reflectometric interference microchip biosensor based on nanoporous alumina for detection of circulating tumour cells. Biosensors and Bioelectronics. 2012;35(1):167-73.
12. Lau KHA, Duran H, Knoll W. In situ Characterization ofN-Carboxy Anhydride Polymerization in Nanoporous Anodic Alumina. The Journal of Physical Chemistry B. 2009;113(10):3179-89.
13. Wang H, Wei M, Zhong Z, Wang Y. Atomic-layer-deposition-enabled thin-film composite membranes of polyimide supported on nanoporous anodized alumina. Journal of Membrane Science. 2017;535:56-62.
14. Gao T, Meng G, Tian Y, Sun S, Liu X, Zhang L. Photoluminescence of ZnO nanoparticles loaded into porous anodic alumina hosts. Journal of Physics: Condensed Matter. 2002;14(47):12651-6.
15. Mei YF, Li ZM, Chu RM, Tang ZK, Siu GG, Fu RKY, et al. Synthesis and optical properties of germanium nanorod array fabricated on porous anodic alumina and Si-based templates. Applied Physics Letters. 2005;86(2):021111.
16. Lu Z, Ruan W, Yang J, Xu W, Zhao C, Zhao B. Deposition of Ag nanoparticles on porous anodic alumina for surface enhanced Raman scattering substrate. Journal of Raman Spectroscopy. 2009;40(1):112-6.
17. Ghugal SG, Mahalik RR, Charde PS, Umare SS, Kokane SB, Sudarsan V, et al. Photocatalytic properties of mesoporous alumina containing Ni doped CdS nanostructures. Microporous and Mesoporous Materials. 2017;242:284-93.
18. Zhang J, Wang S, Wang Y, Xu M, Xia H, Zhang S, et al. Facile synthesis of highly ethanol-sensitive SnO2 nanoparticles. Sensors and Actuators B: Chemical. 2009;139(2):369-74.

19. Wang H, Liang J, Fan H, Xi B, Zhang M, Xiong S, et al. Synthesis and gas sensitivities of SnO2 nanorods and hollow microspheres. Journal of Solid State Chemistry. 2008;181(1):122-9.
20. J. Gajendiran and V. Rajendran, Different surfactants assisted on the synthesis of SnO 2 nanoparticles and their characterization, Int J Mater Biomater Appl, 2012, 2, 37–40.
21. Li X, Chin E, Sun H, Kurup P, Gu Z. Fabrication and integration of metal oxide nanowire sensors using dielectrophoretic assembly and improved post-assembly processing. Sensors and Actuators B: Chemical. 2010;148(2):404-12.
22. Mozalev A, Vazquez RM, Bendova M, Pytlicek Z, Llobet E, Hubalek J. Porous-alumina-Assisted Formation of 3-D Nanostructured Niobium Oxide Films for Advanced Sensing Applications. Procedia Engineering. 2015;120:435-8.
23. Masuda H, Fukuda K. Ordered Metal Nanohole Arrays Made by a Two-Step Replication of Honeycomb Structures of Anodic Alumina. Science. 1995;268(5216):1466-8.
24. Liu Y, Jiao Y, Qu F, Gong L, Wu X. Facile Synthesis of Template-Induced SnO2Nanotubes. Journal of Nanomaterials. 2013;2013:1-6.
25. Lee W, Ji R, Gösele U, Nielsch K. Fast fabrication of long-range ordered porous alumina membranes by hard anodization. Nature Materials. 2006;5(9):741-7.
26. Han CY, Willing GA, Xiao Z, Wang HH. Control of the Anodic Aluminum Oxide Barrier Layer Opening Process by Wet Chemical Etching. Langmuir. 2007;23(3):1564-8.
27. Han H, Park S-J, Jang JS, Ryu H, Kim KJ, Baik S, et al. In Situ Determination of the Pore Opening Point during Wet-Chemical Etching of the Barrier Layer of Porous Anodic Aluminum Oxide: Nonuniform Impurity Distribution in Anodic Oxide. ACS Applied Materials & Interfaces. 2013;5(8):3441-8.
28. Wang H, Liang J, Fan H, Xi B, Zhang M, Xiong S, et al. Synthesis and gas sensitivities of SnO2 nanorods and hollow microspheres. Journal of Solid State Chemistry. 2008;181(1):122-9.